[CANCER RESEARCH 64, 3508–3516, May 15, 2004]

# Loss of Vascular Endothelial Growth Factor A Activity in Murine Epidermal Keratinocytes Delays Wound Healing and Inhibits Tumor Formation

**Heidemarie Rossiter,[1] Caterina Barresi,[1] Johannes Pammer,[2] Michael Rendl,[1,3] Jody Haigh,[4,5] Erwin F. Wagner,[4] and Erwin Tschachler[1]**

*[1]Department of Dermatology, [2]Institute of Clinical Pathology, Medical University of Vienna, Vienna, Austria; [3]Howard Hughes Medical Institute, Laboratory of Mammalian and Cell Biology and Development, The Rockefeller University, New York, New York; [4]Research Institute for Molecular Pathology, Vienna, Austria; and [5]Samuel Lunenfeld Research Institute, Mount Sinai Hospital, Toronto, Canada*

## ABSTRACT

**The angiogenic cytokine vascular endothelial growth factor (VEGF)-A plays a central role in both wound healing and tumor growth. In the skin, epidermal keratinocytes are a major source of this growth factor. To study the contribution of keratinocyte-derived VEGF-A to these angiogenesis-dependent processes, we generated mice in which this cytokine was inactivated specifically in keratin 5-expressing tissues. The mutant mice were macroscopically normal, and the skin capillary system was well established, demonstrating that keratinocyte-derived VEGF-A is not essential for angiogenesis in the skin during embryonic development. However, healing of full-thickness wounds in adult animals was appreciably delayed compared with controls, with retarded crust shedding and the appearance of a blood vessel-free zone underneath the newly formed epidermis. When 9,12-dimethyl 1,2-benzanthracene was applied as both tumor initiator and promoter, a total of 143 papillomas developed in 20 of 23 (87%) of control mice. In contrast, only three papillomas arose in 2 of 17 (12%) of the mutant mice, whereas the rest merely displayed epidermal thickening and parakeratosis. Mutant mice also developed only 2 squamous cell carcinomas, whereas 11 carcinomas were found in seven of the control animals. These data demonstrate that whereas keratinocyte-derived VEGF-A is dispensable for skin vascularization under physiological conditions, it plays an important albeit nonessential role during epidermal wound healing and is crucial for the development of 9,12-dimethyl 1,2-benzanthracene-induced epithelial skin tumors.**

## INTRODUCTION

Vascular endothelial growth factor (VEGF)-A, first described as a vascular permeability factor and subsequently described as an endothelial cell-specific growth factor, is the founding member of a family of VEGFs that includes VEGF-B, VEGF-C, VEGF-D, and placenta growth factor [PlGF (1)]. These additional VEGF family members share receptors with VEGF-A (2); both VEGF-D and PlGF can stimulate angiogenesis (3, 4), whereas VEGF-B is only weakly mitogenic for blood vessel endothelial cells *in vitro* but appears to contribute to cardiac vessel development and function. VEGF-C seems mainly to be a growth factor for lymphatic endothelial cells (5), although it might also play a role in vessel development because VEGF receptor 3-null mice die at midgestation, before the onset of lymphangiogenesis (6). In addition, PlGF can form heterodimers with VEGF-A (7) and may regulate the activity of VEGF-A by competing for their common receptor, VEGF receptor 1 [Flt-1 (8)]. VEGF-A is essential for blood vessel formation during embryonic development (9, 10). In contrast, in the adult organism, where blood vessels are normally quiescent, VEGF-A is up-regulated in settings of increased vascular requirements, such as during the female reproductive cycle, and during tissue repair and tumor growth (for reviews, see Refs. 1, 2, and 11).

In the skin, the main source of VEGF-A is the epidermal keratinocyte. Keratinocytes constitutively express VEGF-A protein (12, 13), and a marked up-regulation of VEGF-A is observed in these cells during wound healing (14) and inflammatory skin diseases (15–17). VEGF-A is also abundantly expressed in epithelial skin tumors (13, 18). However, other sources can contribute to the overall levels of VEGF-A in the skin: the dermal extracellular matrix harbors heparin-bound VEGF-A that can be liberated by proteases activated in a wound bed (reviewed in Ref. 2), and dermal macrophages, migrating into a wound, express VEGF-A mRNA (14). In addition, other cytokines, such as PlGF (4), fibroblast growth factor 2 (19), and the angiopoietins and thrombospondins participate in the regulation of angiogenesis in the skin (20, 21). Finally, in the setting of tumor-mediated angiogenesis, VEGF-A promoter activity was found to be induced in tumor stromal cells (22), suggesting that tumors can regulate angiogenic activity in nontransformed peritumoral cells.

Thus, to examine the relative contribution that keratinocyte-derived VEGF-A makes to pathophysiological angiogenesis in the skin, mice in which VEGF-A is inactivated specifically in epidermal and follicular keratinocytes were generated by means of the Cre-lox-P system (23). Studies on the healing of skin wounds and susceptibility to carcinogen-induced papilloma formation reveal that, depending on the setting of the angiogenic stimulus, epidermal keratinocytes contribute to quite different degrees to blood vessel formation.

## MATERIALS AND METHODS

### Generation of VEGF-A-Deficient Mice

A male mouse bearing the *cre* recombinase transgene under the control of the keratin 5 (K5) promoter [K5-$cre^{+}$ (24)] was mated to females homozygous for the floxed VEGF-A allele [*VEGF-A*$^{loxP/loxP}$ (25); both mouse lines are from a C57Bl/6 × 129 mixed background]. *VEGF-A*$^{\Delta k5\text{-}cre/+}$ $F_1$ heterozygotes (that have deleted one *VEGF-A* allele specifically in K5-cre-expressing cells) were bred to mice homozygous for the *VEGF-A*$^{loxP/loxP}$ allele. Offspring from these matings that have deleted both of the floxed *VEGF-A* alleles specifically in K5-*cre*-expressing cells (*VEGF-A*$^{\Delta k5\text{-}cre/\Delta k5\text{-}cre}$) are designated as mutant mice, and age- and sex-matched *VEGF-A*$^{loxP/loxP}$ animals (littermates as far as possible) served as controls. Unless otherwise noted, all mice were 7–8 weeks of age when analyzed or used for experiments.

### PCR and Southern Blotting

PCR and Southern blotting were performed on genomic DNA from tail epidermal sheets prepared by the trypsin flotation method [1 h at 37°C, 0.25% trypsin (Difco 1:250, Detroit, MI) in PBS]. Primers and reaction conditions to detect the LoxP sites, the *cre* transgene, and the recombination efficiency at the *LoxP* sites of the floxed exon 3 of *VEGF-A* have been described previously (25). Here, we have modified the PCR conditions for the detection of recombination by using the primer pair VEGFc5R.2 and mVEGF322.F (Fig. 1; Ref. 25) to detect excision of the entire *VEGF-A* exon 3 by PCR (1 cycle of 95°C for 5 min; 30 cycles of 95°C for 1 min, 58°C for 1 min, and 72°C for 2 min; and 1 cycle of 72°C for 5 min). To confirm the deletion of *VEGF-A* exon 3 by

Received 8/19/03; revised 3/3/04; accepted 3/5/04.

**Grant support:** Grant F511 from the Fond zur Förderung der Wissenschaftlichen Forschung; Centre de Recherches et d'Investigations Épidermiques et Sensorielles, Neuilly, France (H. Rossiter, C. Barresi, J. Pammer, M. Rendl, and E. Tschachler); and Boehringer-Ingelheim, Germany (J. Haigh and E. F. Wagner).

The costs of publication of this article were defrayed in part by the payment of page charges. This article must therefore be hereby marked *advertisement* in accordance with 18 U.S.C. Section 1734 solely to indicate this fact.

**Requests for reprints:** Erwin Tschachler, Deptartment of Dermatology, Medical University of Vienna, Währingergürtel 18-20, A-1090 Vienna, Austria. Phone: 43-1-4081271; Fax: 43-1-4034922; E-mail: erwin.tschachler@akh-wien.ac.at.

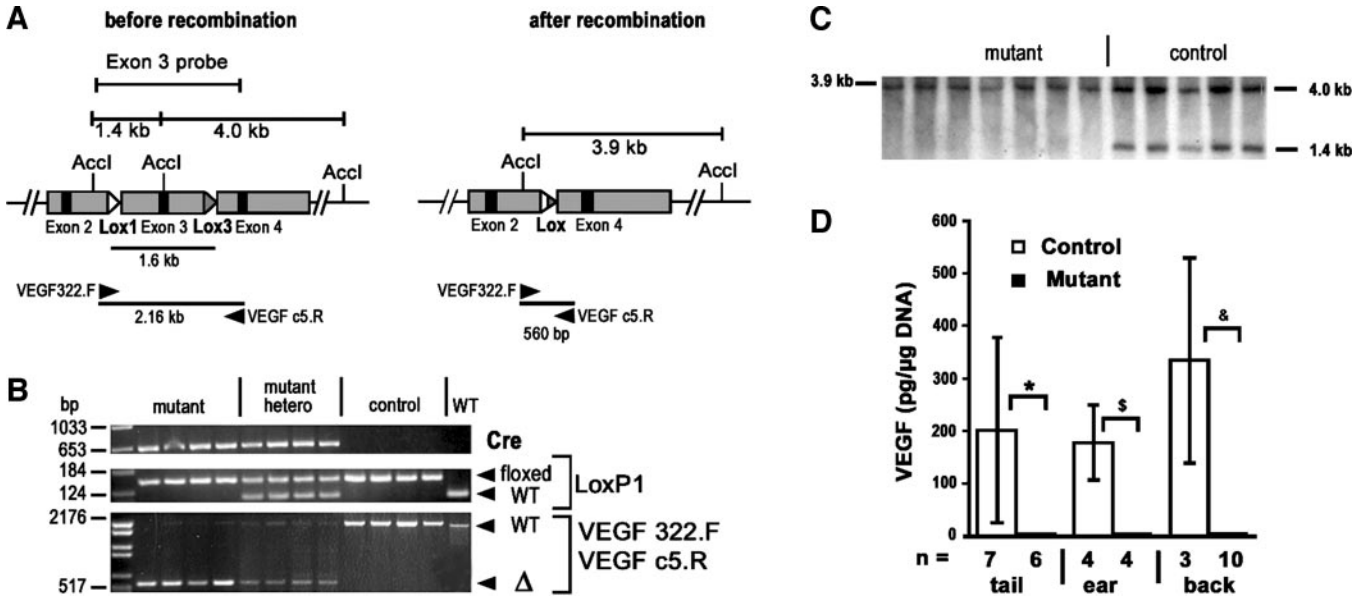


Fig. 1. Cre-mediated recombination of *VEGF-A* exon 3 completely abolishes vascular endothelial growth factor (VEGF)-A secretion by epidermal cells. *A*, position of PCR primers and probe for Southern blotting used to detect excision of *VEGF-A* exon 3. *B*, PCR amplification of epidermal cell genomic DNA using the primer pairs indicated to the *right* of the figure. *mutant*, transgenic for keratin 5 (K5)-*cre* and homozygous for the floxed *VEGF-A* allele; *mutant hetero*, transgenic for K5-*cre* and heterozygous for the floxed *VEGF-A* allele; *control*, nontransgenic for K5-*cre* and homozygous for the floxed *VEGF-A* allele; *WT*, wild-type allele of *VEGF-A* and nontransgenic for K5-*cre*. *C*, Southern blot of similar DNA preparations as described in *B*, using the probe indicated in *A*. Each lane in *B* and *C* represents DNA from an individual mouse. *D*, detection of VEGF-A in supernatants of cultured epidermal cells from the body sites indicated. *n*, number of mice in each group. ∗, $, and &, $P < 0.05$, 0.02, and 0.0005, respectively, for mutant compared with control.

Southern blotting, genomic DNA was digested with ACC I (Roche, Vienna, Austria), separated by agarose gel electrophoresis, and probed with a PCR fragment generated by the primer pair VEGFc5R.2 and mVEGF322.F that spans exon 3 (Fig. 1*A*).

### Tissue Preparation and Cell Culture

To detect VEGF-A production by epidermal keratinocytes, single cell suspensions were prepared from tail or trunk skin of adult or neonatal mice, respectively, by protease digestion. The cells were suspended in low-calcium growth medium (26) and plated at about 80% confluence in Costar 12-well plates coated with collagen IV (Vitrogen, Palo Alto, CA). After initial overnight incubation, adherent cells were cultured for an additional 48 h, and VEGF-A concentrations were assayed by ELISA in cleared supernatants, using a commercial murine VEGF-A ELISA (R&D, Wiesbaden-Nordenstadt, Germany). For some experiments, epidermal sheets prepared from split ears by flotation on dispase solution were used instead of single cell suspensions. Genomic DNA was prepared for quantitation of cell material in each well.

### Histology

Rat antimurine CD31 monoclonal antibody (PharMingen, San Diego, CA) was used to detect blood vessels in either acetone-fixed frozen sections (10 $\mu$g/ml) or dermal sheet preparations from ears (25 $\mu$g/ml). The biotinylated secondary antibody for CD31 staining (Amersham, Little Chalfont, United Kingdom) was used for frozen sections at a dilution of 1:200, whereas for dermal sheets, a phycoerythrin-conjugated secondary antibody (Alexa-Fluor; Molecular Probes, Eugene, OR) was used (4 $\mu$g/ml, final concentration). To detect apoptotic cells, 4-$\mu$m sections of formalin-fixed paraffin-embedded tissues were stained with rabbit antibody to active caspase 3 (R&D Systems, Minneapolis, MN), whereas macrophages were identified with a goat antibody to Mac-1 (anti-integrin $\alpha_M$; Santa Cruz Biotechnology, Heidelberg, Germany). Biotinylated antirabbit and antigoat secondary antibodies were from Vector (Burlingame, CA) for immunohistochemistry or from Molecular Probes (Alexa-Fluor488 or Alexa-Fluor546) for immunofluorescence. Binding of antibodies for immunohistochemistry was visualized with the horseradish peroxidase-strept-ABC from DAKO (Glostrup, Denmark). Additional sections were also stained with H&E or with chloroacetate esterase by standard procedures.

For whole mount blood vessel preparations, dermal sheets recovered after flotation of split ears on 3.8% ammonium isothiocyanate at 37°C for 30–40 min were fixed in acetone for 10 min at 4°C. They were then blocked with a mixture of 10% normal goat serum and 2% BSA in PBS for 60 min, incubated with anti-CD31 antibody overnight at 4°C, and washed twice, and bound antibody was detected by incubation with secondary antibody for 60 min at room temperature. Finally, the preparations were mounted with Fluoprep (bioMérieux, Marcy d'Etoile, France) for microscopic evaluation.

### Wounding Experiments

Three male mice/genotype and time point were depilated with a commercial cream (Veet; Reckitt Benckiser, Mannheim, Germany) 1–2 days before wounding. The mice were anesthetized with 2.5% Avertine (tribromoethyl alcohol/tertiary amyl alcohol; Sigma), and two 6-mm full-thickness punch biopsy wounds were set by folding the back skin and punching through 2 thicknesses of skin. Wounds were measured in two dimensions with handyman's calipers (Metrica) and photographed at the indicated times. At harvest, the animals were sacrificed by chloroform inhalation, and the wounds were excised, bisected, and frozen in OCT compound (Sakura, Zoeterwoude, the Netherlands).

### Carcinogenesis Protocol

A concentration of 50 $\mu$g/50 $\mu$l 9,12-dimethyl 1,2-benzanthracene (DMBA; Sigma) was applied to the backs of 28 *VEGF-A*$^{loxP/loxP}$ and 20 *VEGF-A*$^{\Delta k5\text{-}cre/\Delta k5\text{-}cre}$ mice (1–4 days old) once a week for 17 weeks. The carcinogen was diluted in ethanol for the first eight applications, and then diluted in acetone, and mice were shaved with clippers as needed. Papillomas were scored when they reached a size of 1 mm and had been present for 1 week or more, and at sacrifice, samples of skin and/or tumors were embedded in OCT or fixed in 4.5% formalin and embedded in paraffin (22 control and 13 mutant mice survived to the end of the experiment). Dysplasia was classified in two grade categories. Low-grade intraepithelial dysplasia and reactive simulants, which are not reliably distinguishable from low-grade dysplasia, *i.e.*, atypia, indefinite for dysplasia, consisted of basally located cells with slightly to moderately enlarged or hyperchromatic nuclei involving less than one-half of the epithelium (grade I). By contrast, high-grade dysplasia was composed either of immature cells with distinctly hyperchromatic nuclei involving more than half of the epithelium or of larger basal cells with marked atypical nuclei

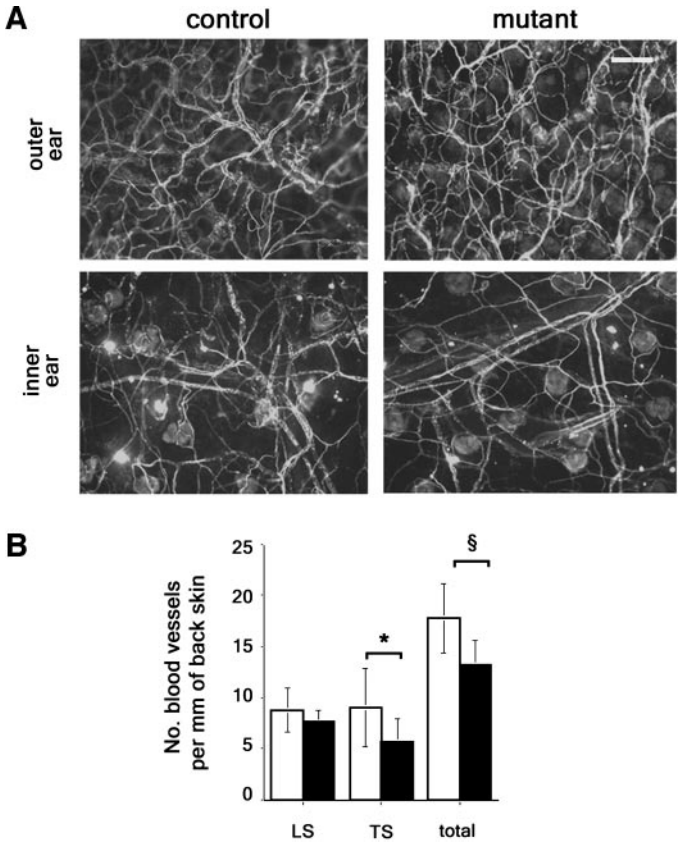


Fig. 2. Blood vessel density in untreated dermis of adult mice. *A*, dermal sheet preparations from ear, stained with CD31. *Bar*, 160 $\mu$m. *B*, blood vessel count/mm back skin on tissue sections. $CD31^+$ structures within 40 $\mu$m of the basal membrane were counted as capillaries cut longitudinally (*LS*) or transversely (*TS*). □, control (*VEGF-*$A^{loxP/loxP}$); ■, mutant (*VEGF-*$A^{\Delta k5\text{-}cre/\Delta k5\text{-}cre}$). ∗, $P < 0.05$; §, $P < 0.001$ for control compared with mutant capillaries cut transversely and in total capillaries, respectively. A total of 3–14 fields of view at ×200 magnification were counted for each of 13 mice/group, averaged, and converted to number of vessels/mm skin.

with irregularly dispersed chromatin but with abundant cytoplasm of superficial cells and para- or hyperkeratosis (grade III).

### Morphometric Analyses of Blood Vessels

**Normal Skin.** The blood vessel density within 40 $\mu$m of the basement membrane of healthy adult skin was assessed in CD31-stained tissue sections by manually counting multicellular and single-celled stained structures over the whole length of the specimen and converting to number of vessels/mm (six control and nine mutant mice were analyzed). Blood vessels immediately adjacent to hair follicles were not included in the counts, and mice in anagen were omitted from the analysis.

**Wounds.** CD31-stained tissue sections were photographed with an RT slider spot digital camera (Visitron, Puchheim, Germany) attached to an Olympus Provis microscope. Calibration of each image and assessment of distances were performed with the Metamorph Imaging System, Version 4.5r3. The distances of blood vessels from the neoepidermis were measured across the entire width of six wounds (on three animals) per genotype for day 8 and 3–4 wounds per genotype for day 23.

**Tumors and Tumor-Free, DMBA-Treated Skin.** Images of CD31-stained tissue sections were captured as described above, and the relative area of blood vessels in the tumor stroma, in the dermis between the rete ridges of hyperplastic skin, or within 100 $\mu$m of the basal membrane in normal skin was calculated using an area tool in Adobe Photoshop 5.5 software. Two squamous cell carcinomas (SCCs), three papillomas (all on different mice), tumor-free DMBA-treated skin from three control mice, and DMBA-treated skin from six mutant mice, with 2–3 images/sample, were used for quantitation.

Student's *t* test was used to analyze the statistical significance of all groups compared.

## RESULTS

**Loss of *VEGF-A* Exon 3 Inhibits VEGF-A Secretion by Epidermal Keratinocytes.** Mice were genotyped by PCR amplification of tail DNA. (Fig. 1, *A* and *B*). *Cre*-specific primers detect the presence of the *cre* transgene (Fig. 1*B, top panel*), whereas primers that flank the loxP1 insertion site distinguish *VEGF-*$A^{loxP/loxP}$ homozygotes (PCR product of 150 bp only; Fig. 1*B, middle panel*) from *VEGF-*$A^{loxP/+}$ heterozygotes (PCR products of 100 and 150 bp) and *VEGF-*$A^{+/+}$ wild-type mice (100 bp only). Finally, amplification of DNA from epidermal cell preparations with primers that bind to either side of *VEGF-A* exon 3 demonstrates the efficient excision of this stretch of DNA in *VEGF-*$A^{\Delta k5\text{-}cre/\Delta k5\text{-}cre}$ mice, but not in *VEGF-*$A^{loxP/loxP}$ mice (Fig. 1*B, bottom panel*, bands of 560 bp and 2.1 kb, respectively).

Excision of *VEGF-A* exon 3 in epidermal cell preparations was confirmed by Southern blotting. The probe used for hybridization spans an *Acc*I site that is lost if excision of *VEGF-A* exon 3 takes place (Fig. 1*A*). The results of a representative Southern hybridization, shown in Fig. 1*C*, confirm that the expected bands of 1.4 and 4.0 kb are obtained with keratinocyte DNA from *VEGF-*$A^{loxP/loxP}$ mice, whereas every *VEGF-*$A^{\Delta k5\text{-}cre/\Delta k5\text{-}cre}$ mouse tested shows the expected band of 3.9 kb (each lane, for both PCR and Southern blot, represents an individual mouse).

Attempts to demonstrate decreased VEGF-A protein production in the mutant mice *in vivo* by immunohistochemical analysis of normal skin and wounds were unsuccessful; both mutant and control mice stained equally well (data not shown). Because all of the commercially available antibodies are directed against the $NH_2$ terminus of the protein, they must recognize a truncated product in the mutant mice. However, Fig. 1*D* shows that using a sensitive ELISA assay, no VEGF-A protein could be detected in the supernatants of cultured epidermal cells from various body sites of *VEGF-*$A^{\Delta k5\text{-}cre/\Delta k5\text{-}cre}$ mice. Note that of the four ear preparations, two were cultures of dispersed epidermal cells, and two were cultures of intact epidermal sheets from split ears. Thus, K5-*cre*-mediated excision of VEGF-A exon 3 is efficient, and epidermal keratinocytes of mutant mice do not secrete detectable amounts of VEGF-A into culture medium. Furthermore, no compensatory up-regulation of PlGF protein was found by ELISA in similar supernatants, nor was compensatory up-regulation of PlGF mRNA found in epidermal cells by quantitative reverse transcription-PCR (not shown).

**Mutant Mice Are Grossly Normal and Exhibit Only a Slight Reduction in Subepidermal Capillary Density.** Mutant pups were born at approximately the expected Mendelian frequencies, as long as male K5-$cre^+$ mice were used for transgene transmission. In contrast, when female *VEGF-*$A^{\Delta k5\text{-}cre/\Delta k5\text{-}cre}$ mice were used for breeding, they bore fewer young than controls, and all offspring lacked the K5-*cre* transgene. Presumably, germ-line excision of the floxed *VEGF-A* allele due to global zygotic gene activation (27) results in lethality at midgestation (9, 10).

Mutant newborn pups were healthy and had no obvious skin defects, but mutant males grew more slowly than controls and weighed 10–20% less between weeks 2 and 8 of age [$P < 0.05$ at weeks 2–3 and 5–8 (data not shown)]. Thereafter, all male mice were of similar weight. Interestingly, mutant females were significantly smaller only at 5–6 weeks and >12 weeks of age. For each genotype and time point, a minimum of 3 mice (up to a maximum of 19 mice, depending on availability) were weighed. Although angiogenesis and/or VEGF-A production by keratinocytes has been reported to be regulated in concert with the hair cycle (28, 29), we observed that macroscopically, the onset of the first hair cycle occurred simultaneously in mutant and control mice, and no overt hair abnormalities were

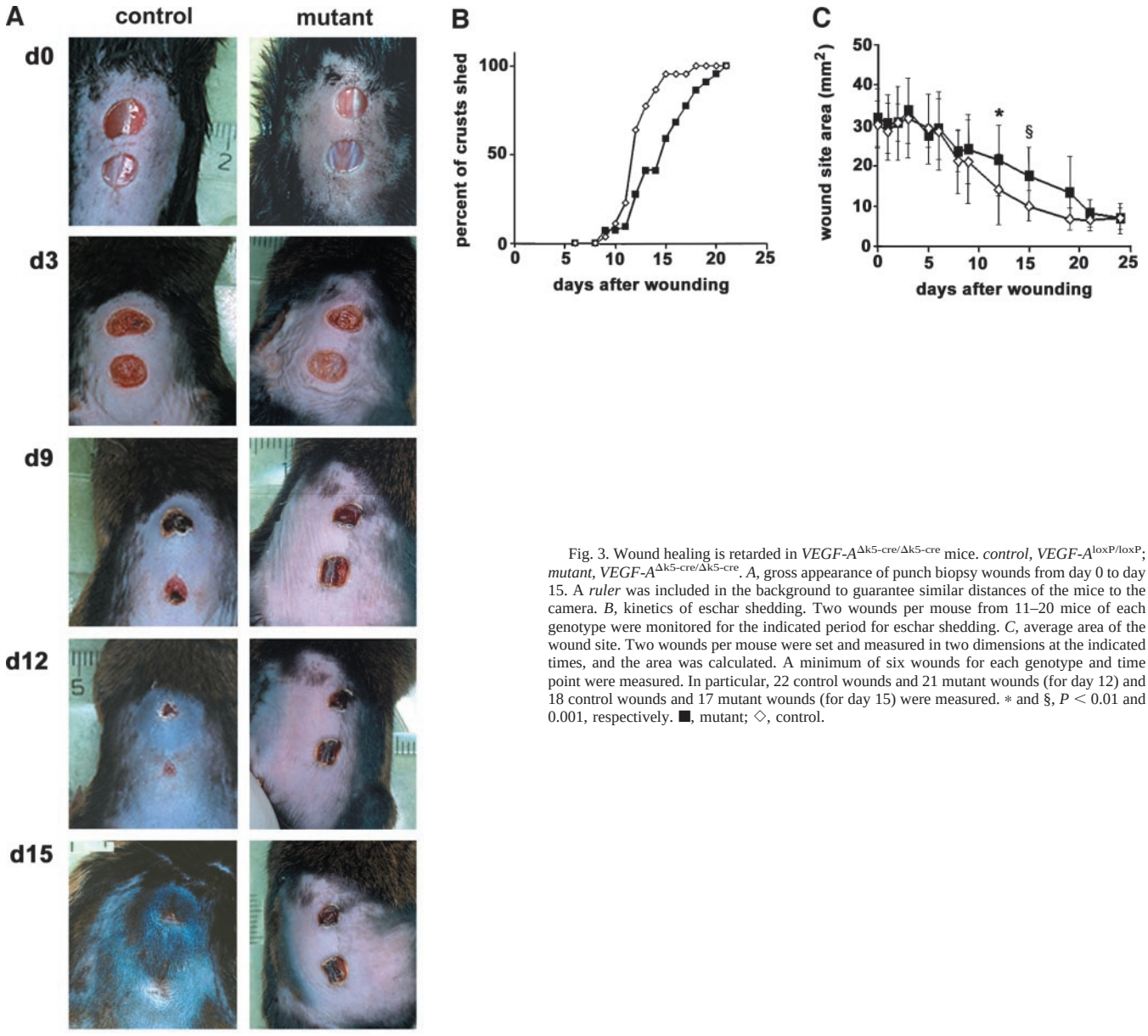


Fig. 3. Wound healing is retarded in *VEGF-A*$^{\Delta k5\text{-}cre/\Delta k5\text{-}cre}$ mice. *control*, *VEGF-A*$^{loxP/loxP}$; *mutant*, *VEGF-A*$^{\Delta k5\text{-}cre/\Delta k5\text{-}cre}$. *A*, gross appearance of punch biopsy wounds from day 0 to day 15. A *ruler* was included in the background to guarantee similar distances of the mice to the camera. *B*, kinetics of eschar shedding. Two wounds per mouse from 11–20 mice of each genotype were monitored for the indicated period for eschar shedding. *C*, average area of the wound site. Two wounds per mouse were set and measured in two dimensions at the indicated times, and the area was calculated. A minimum of six wounds for each genotype and time point were measured. In particular, 22 control wounds and 21 mutant wounds (for day 12) and 18 control wounds and 17 mutant wounds (for day 15) were measured. ∗ and §, $P < 0.01$ and 0.001, respectively. ■, mutant; ◇, control.

observed in the mutant mice up to an age of 2 years (data not shown). A preliminary histomorphometric analysis of the first hair cycle revealed that, compared with controls, hair follicles in mutant mice entered catagen earlier, and there was a reduced interfollicular microvessel density between days 6 and 19.[6] However, a detailed analysis of the hair cycle in these mice is beyond the scope of the present study.

Whole mount CD31 staining of normal ear dermis revealed no apparent differences in densities of larger blood vessels between mutant and control mice (Fig. 2*A*). However, enumeration of CD31-stained microvessels in frozen sections revealed a small but significant reduction in the number of capillaries lying within 40 $\mu$m of the basement membrane (Fig. 4*K*) in the mutant mice compared with controls (Fig. 2*B*). Thus, the absence of keratinocyte-derived VEGF-A has only a marginal effect on the vasculature of quiescent skin.

**Wound Healing Is Retarded in *VEGF-A*$^{\Delta k5\text{-}cre/\Delta k5\text{-}cre}$ Mice.** Because angiogenesis is necessary for effective tissue repair, we asked whether the lack of VEGF-A production by epidermal keratinocytes in *VEGF-A*$^{\Delta k5\text{-}cre/\Delta k5\text{-}cre}$ mice would affect the healing of skin wounds. Fig. 3*A* shows that the initial phase of clotting and crust formation proceeded similarly in both mutant and control groups. However, after about day 6, crust shedding stagnated in mutant mice, and wounds were still covered with a crust by day 12, a time at which control wounds had almost healed. Fig. 3*B* shows that 50% of the crusts are shed by day 11 after wounding in the *VEGF-A*$^{loxP/loxP}$ mice compared with day 15 in the mutant mice, and mutant wounds are significantly larger at days 12 and 15 (Fig. 3*C*).

Because wound healing during the first 9 days progressed comparably in both mutant and control mice, the wounds were examined microscopically at time points just preceding the observed macroscopic differences (days 6–10). At day 6, wounds in both groups appeared similar: newly formed epidermis (*asterisk*) can be seen dissecting under the fibrin clot (Fig. 4, *A* and *B*), and the granulation tissue of both groups displays rich neovascularization, as visualized by CD31 staining. By day 8, blood vessel density was still high in the hypercellular granulation tissue at the wound center (Fig. 4, *C* and *D*) but had started to decline at the wound periphery, and an avascular zone had appeared adjacent to the basement membrane of the neo-

[6] L. Mecklenburg and R. Paus, unpublished observations.

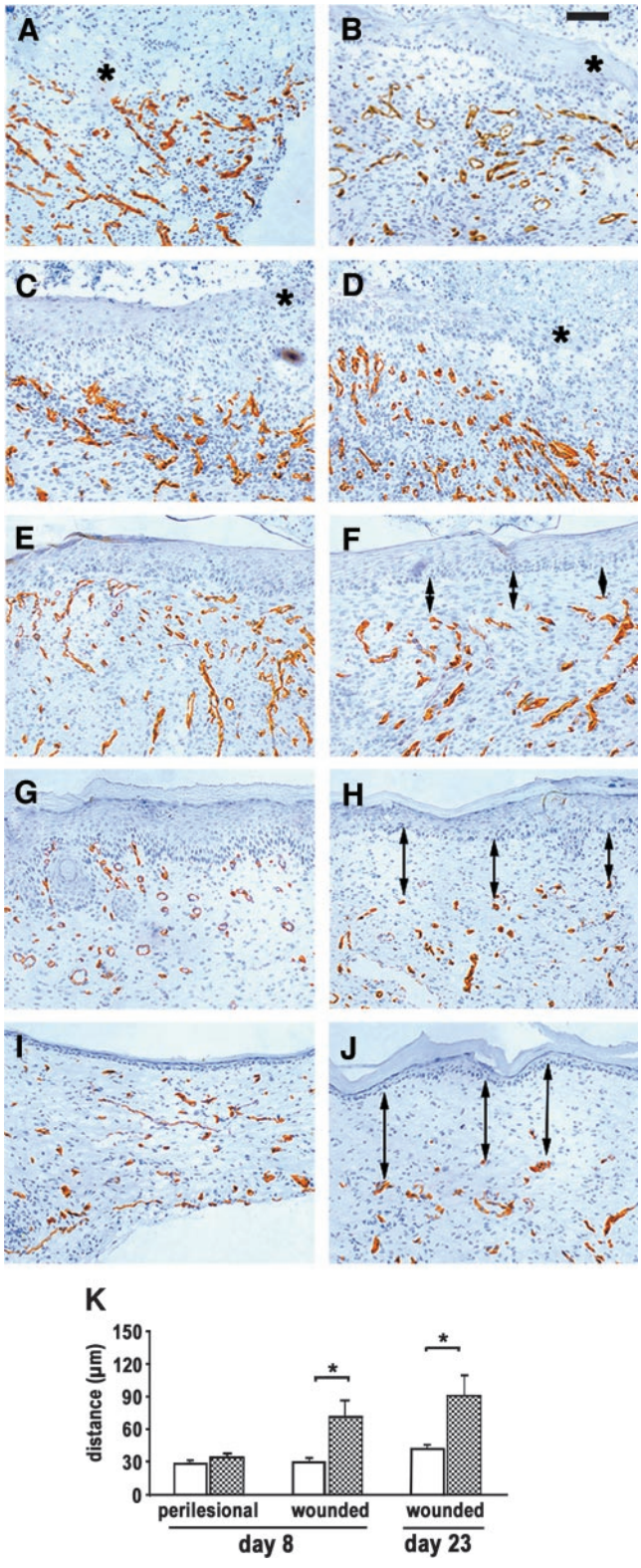


Fig. 4. *VEGF-A*$^{\Delta k5\text{-}cre/\Delta k5\text{-}cre}$ mice develop a subepidermal avascular zone in healing wounds. CD31-stained cryosections of representative wounds from day 6 (*A* and *B*); day 8, wound center (*C* and *D*); day 8, wound periphery of the same wound as in *C* and *D* (*E* and *F*); day 10 (*G* and *H*); and day 23 (*I* and *J*) show that a blood vessel-free zone develops beneath the newly formed epidermis in *VEGF-A*$^{\Delta k5\text{-}cre/\Delta k5\text{-}cre}$ (mutant) mice (*B, D, F, H,* and *J*), but not in *VEGF-A*$^{loxP/loxP}$ (control) mice (*A, C, E, G,* and *I*). *Bar,* 35 $\mu$m. The distance of the nearest blood vessels (defined as structures strongly staining for CD31) from the neoepidermis of the wound is greater in mutant mice than in controls (*K*). Blood vessels along the total wound length of six wounds from three mice of each genotype were quantitated for day 8, and three to four wounds on two mice of each genotype were quantitated for day 23. □, control mice; ▨, mutant mice. $P < 0.005$ for each of the wound time points for control compared with mutant mice.

epidermis in the mutant mice, but not the control mice (Fig. 4, *E* and *F*, wound margins of same wounds as shown in Fig. 4, *C* and *D*). Apart from the lack of blood vessels, this area appeared similar in both groups of mice, and was composed of highly cellular, fibronectin-rich granulation tissue in the earlier wounds (up to day 10), which was replaced by relatively acellular collagenous dermis by day 14 (data not shown). This blood vessel-free zone is retained in the mutant mice at all subsequent time points examined (at 2-day intervals up to day 23 after wounding; days 10 and 23 are shown, Fig. 4, *G–J*).

Histomorphometric analysis of the location of blood vessels revealed that these lie significantly further away from the basal membrane in mutant mice compared with controls (days 8 and 23 are shown as representative of open and completely healed wounds). Vessels in unwounded skin, however, were situated at similar distances from the basal membrane in both groups (Fig. 4*K*).

Because macrophages can also secrete VEGF-A and are often recruited to sites of active angiogenesis, we examined the distribution of Mac-1-positive cells in wounds from day 6 to day 19 and in uninvolved peri-wound skin. Whereas similar numbers of Mac-1-positive cells were found in the upper dermis of peri-wound skin ($2.95 \pm 1.2$ and $2.50 \pm 0.6$ cells/mm epidermis of mutant and control mice, respectively; $P > 0.05$; $n = 2$ mice; 15 fields of view/genotype), their numbers varied greatly in wounds, appearing to be more numerous in mutant granulation tissue of day 6 wounds ($261.0 \pm 87.5$ and $90.4 \pm 25.2$ cells/mm$^2$, respectively; $P < 0.005$; $n = 4$ mutant and 3 control wounds). In healed wounds at days 14–19, Mac-1-positive cells were mostly in the deeper dermis in all mice, with occasional cells near the basal membrane (and thus in the avascular zone in the case of mutant mice), but there was no apparent correlation with the presence of keratinocyte-derived VEGF-A or with blood vessel density. Wound healing is thus retarded in the mutant mice and associated with the appearance of a blood vessel-free zone adjacent to the neoepidermis.

**Papilloma Development Is Abrogated in DMBA-Treated *VEGF-A*$^{\Delta k5\text{-}cre/\Delta k5\text{-}cre}$ Mice.** In a preliminary experiment, adult female mice of the strain used in this study (C57Bl6 × 129) were almost completely refractory to squamous papilloma development induced by initiation with $2 \times 50$ $\mu$g of DMBA and promotion with 5 $\mu$g of phorbol 12-myristate 13-acetate for 20 weeks (data not shown). However, in subsequent experiments, commencing DMBA treatment when mice were 1–4 days of age and continuing for 17 weeks, 1–20 papillomas/mouse developed. A total of 143 papillomas developed in 20 of 23 (87%) control animals, whereas only 3 papillomas were found in 2 of 17 mutant mice (Table 1; Fig. 5 *A*).

Male *VEGF-A*$^{loxP/loxP}$ mice were more sensitive to papilloma induction than *VEGF-A*$^{loxP/loxP}$ females: they developed more lesions, that appeared earlier; and all of the male (but only 70% of the female) control mice had papillomas for at least some of the time (Fig. 5*B*). Many of the mice (both mutant and controls) appeared moribund at about 20 weeks after the start of DMBA application, and histological analysis of spleen, liver, and lung of these mice revealed lymphoma-like infiltrates (data not shown).

Histological examination of H&E-stained, formalin-fixed sections of the tumors of control mice revealed that the majority of skin lesions were typical squamous papillomas (Fig. 6, *A* and *C*; Table 1) In addition, 11 SCCs of grade I–III (30) were identified in 7 control animals (Fig. 6, *B* and *D*), and only 1 carcinoma was identified in each of 2 of the mutant mice. Both mutant and control mice displayed epidermal hyperplasia in the area of DMBA application, but these changes were much more severe in the mutants (Fig. 5*A*) than in the controls (data not shown). Indeed, the treated skin of mutant mice showed evidence of either abundant inflammatory cells (Fig. 6, *G* and *I*), or a hyperproliferative epidermis and a parakeratotic stratum cor-

Table 1 *DMBA[a] induces many tumors in VEGF-A$^{loxP/loxP}$[b] but not in VEGF-A$^{\Delta k5\text{-}cre/\Delta k5\text{-}cre}$[c] mice*

Mice were treated on their shaved backs with DMBA (50 $\mu$g/50 $\mu$l solvent) for 17 weeks, starting at 1–4 days of age, and monitored weekly for 25 weeks. The solvent for DMBA was ethanol for the first 8 weeks and acetone for the remaining time.

| | *VEGF-A*$^{loxP/loxP}$ | | *VEGF-A*$^{\Delta k5\text{-}cre/\Delta k5\text{-}cre}$ | |
|---|---|---|---|---|
| Genotype | Males | Females | Males | Females |
| No. of mice surviving to the end of the experiment/number of mice initially | 13/13 | 10/11 | 8/9 | 9/11 |
| No. of mice with papillomas/number of mice surviving to week 25. | 13/13 | 7/10 | 0/8 | 2/9 |
| No. of papillomas | 102 | 41 | 0 | 3 |
| No. of carcinomas | 6 | 5 | 1[d] | 1 |

[a] DMBA, 9,12-dimethyl 1,2-benzanthracene; VEGF, vascular endothelial growth factor.
[b] *VEGF-A*$^{loxP/loxP}$: mice homozygous for the floxed exon 3 of the *VEGF-A* gene.
[c] *VEGF-A*$^{\Delta k5\text{-}cre/\Delta k5\text{-}cre}$: mice homozygous for the floxed exon 3 of the *VEGF-A* gene and transgenic for Keratin 5-cre.
[d] This carcinoma arose *de novo*, without prior papilloma formation.

neum (Fig. 6, *H* and *J*). The lack of keratinocyte-derived VEGF-A may allow enhanced binding of keratinocyte-derived PlGF to VEGF-A receptor 1, resulting in an increase in inflammatory cell recruitment to the DMBA-treated skin (31), which could exacerbate epidermal hyperproliferation (32). Control mice showed low- to high-grade dysplasia in papillomas and carcinomas, respectively (Fig. 6*C*, *arrows*; Fig. 6*D*, most cells). In contrast, although 12 of 13 mutant mice that were examined histologically displayed epidermal hyperplasia, even the most hyperplastic sections were free of evidence of neoplastic change and only showed evidence of low-grade dysplasia or were indefinite for dysplasia (Fig. 6*J*). p53 protein was only detected in one specimen (from a mutant mouse; data not shown), in agreement with previous findings that this is not the primary mutation induced by DMBA.

CD31 staining of frozen sections revealed an ample supply of large blood vessels in intimate contact with the basal keratinocyte layers of the tumors in the control mice (Fig. 6, *E* and *F*). In contrast, the blood vessels situated near the hyperplastic epidermis in the mutant mice were thin and delicate-looking (compare Fig. 6*E* with Fig. 6, *K* and *L*). Quantitative histomorphometric analysis of blood vessel area in the tumor stroma of control mice or the dermis between the psoriasiform hyperplastic epithelial projections of mutant mice showed that the former occupied a significantly larger area than the latter and was in fact similar to the area occupied by blood vessels in uninvolved control dermis (Fig. 6*M*). In addition, large s.c. vessels emanating from papillomas in the control mice (Fig. 7, *A* and *C*) were missing underneath the treated skin of the mutant mice (Fig. 7, *B* and *D*).

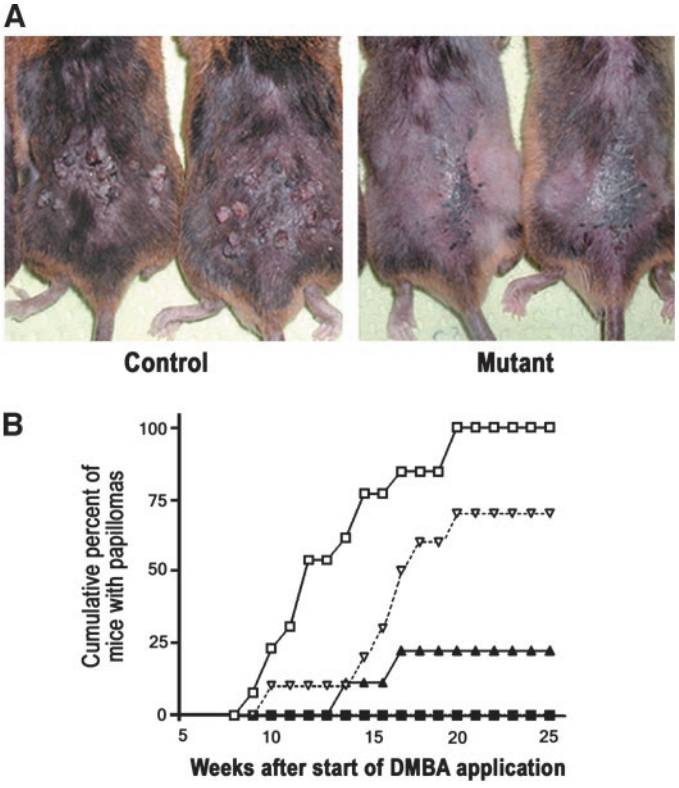


Fig. 5. *VEGF-A*$^{\Delta k5\text{-}cre/\Delta k5\text{-}cre}$ mice develop virtually no tumors in response to 9,12-dimethyl 1,2-benzanthracene. *A*, physical appearance of treated skin of control (*left panel*) and mutant (*right panel*) mice 20 weeks after the beginning of 9,12-dimethyl 1,2-benzanthracene application. *B*, percentage of mice developing papillomas with respect to time. □, male controls; ▽, female controls; ■, male mutants; ▲, female mutants.

Inflammatory cells are attracted to sites of hyperplasia and dysplasia and are thought to contribute to the angiogenic switch (33), a prerequisite for tumor growth. Thus, to examine whether a reduced infiltration of inflammatory cells could contribute to the decreased blood vessel density in the mutant mice, sections of DMBA-treated skin, as well as SCCs and papillomas from controls, were stained with chloroacetate esterase to detect mast cells and neutrophils (2 DMBA-treated, tumor-free skin samples; 2 papillomas and 2 SCCs from control mice; and 6 DMBA-treated skin samples from mutant mice) and Mac-1 to detect macrophages (4 DMBA-treated, tumor-free skin samples; 2 papillomas and 2 SCCs from control mice; and 7 DMBA-treated skin samples from mutant mice). Normal-appearing DMBA-treated skin of both genotypes harbored few cells of either type ($4.0 \pm 0.2$ compared with $6.5 \pm 1.5$ mast cells/mm for control and mutant mice, respectively). Many mast cells ($37 \pm 16$ cell/mm) were, however, located adjacent to the hyperplastic epidermis of mutant mice, but not near SCCs ($3.8 \pm 2.1$ cells/mm), papillomas, or moderately hyperplastic epidermis of controls ($12 \pm 10$ cells/mm; $P < 0.0001$). Macrophages were plentiful in the inflamed dermis of mutant mice and, as expected, in SCCs and papillomas of controls (data not shown).

The reduced blood vessel density found in the mutant mice could result in a reduction of nutrient supply to the epidermis, leading to increased cell death, thereby preventing papilloma outgrowth. However, when we tested for the presence of apoptotic cells by immunostaining for activated caspase 3, no significant difference was found between hyperproliferative epidermis of mutant mice compared with the DMBA-treated skin of controls ($1.14 \pm 1.27$ and $1.22 \pm 1.24$ cells/mm epidermis, respectively; $n = 5$ control and 7 mutant mice).

Thus, virtually no tumors form in DMBA-treated skin of *VEGF-A*$^{\Delta k5\text{-}cre/\Delta k5\text{-}cre}$ mice, and blood vessel density does not increase, despite the presence of dermal cells that could provide angiogenic factors. Furthermore, the lack of tumor formation is not associated with increased apoptosis in the carcinogen-treated skin.

## DISCUSSION

The conditional inactivation of VEGF-A specifically in epidermal keratinocytes has allowed us to examine the functional contribution of VEGF-A produced by these cells to angiogenesis during wound

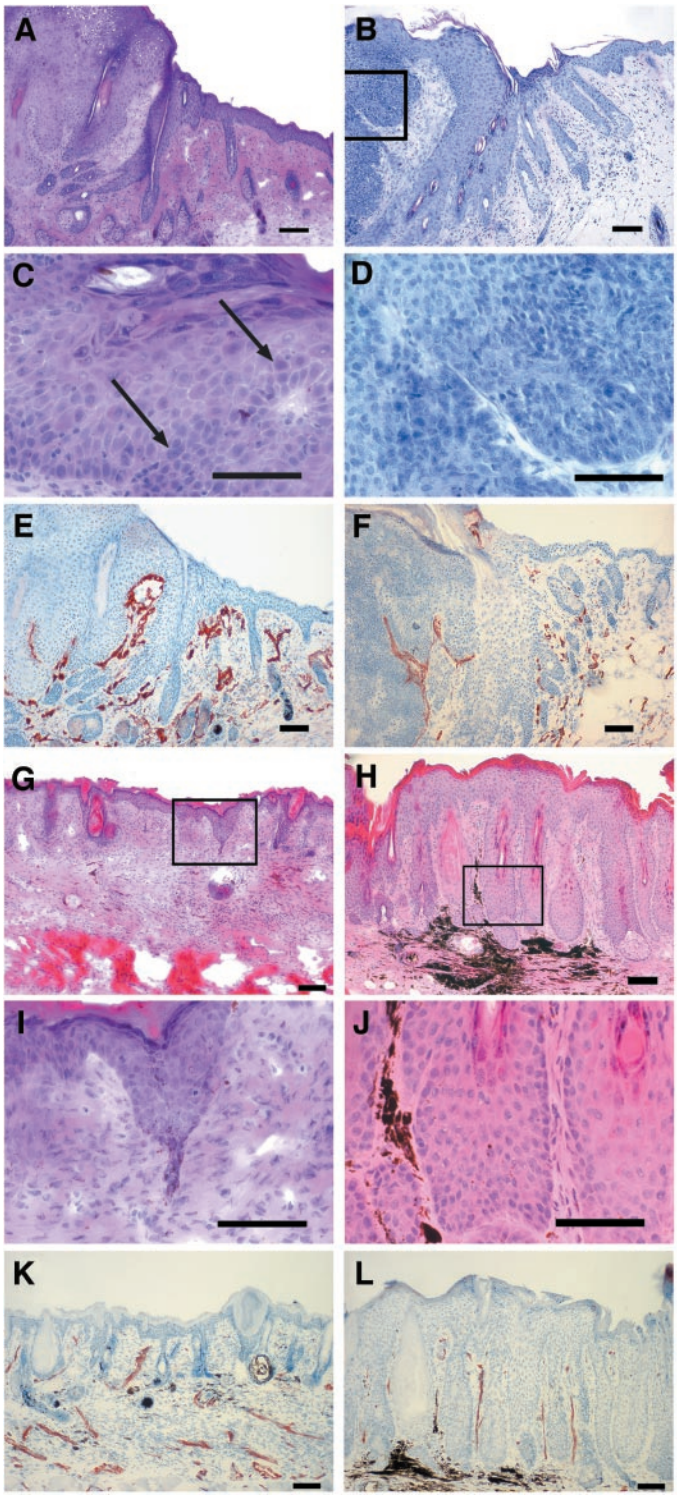


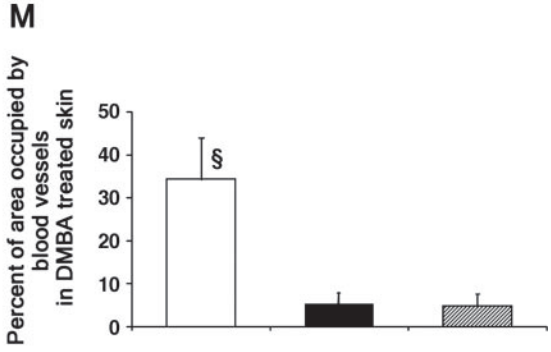


Fig. 6. The 9,12-dimethyl 1,2-benzanthracene (DMBA)-treated skin of *VEGF-A*$^{\Delta k5\text{-cre}/\Delta k5\text{-cre}}$ mice harbors virtually no dysplastic cells and displays reduced blood vessel area. Representative papilloma (*A*, *C*, and *E*) and squamous cell carcinoma (*B*, *D*, and *F*) from a control mouse stained with H&E (*A–D*), and CD31 (*E* and *F*). Peritumoral epidermis exhibits nearly normal morphology, with little inflammation. Inflamed (*G*, *I*, and *K*) and acanthotic (*H*, *J*, and *L*) skin from two different mutant mice stained with H&E (*G–J*), and CD31 (*K* and *L*). *C* and *D*, interior of the papilloma. *Boxed* areas in *B*, *G*, and *H* are shown enlarged in *D*, *I*, and *J*, respectively. The dysplastic cells shown enlarged in *C* (*arrows*) were found in the same papilloma shown in *A*, but more towards the center of the tumor. Nearly all cells in the squamous cell carcinoma (*D*) are dysplastic. *I* and *J* depict higher power views of the same sections as *G* and *H*, showing inflammatory cell infiltrates and lack of dysplasia. *Bar*, 35 $\mu$m. CD31-stained blood vessels occupy a significantly smaller area in DMBA-treated psoriasiform skin of mutant mice compared with peritumoral stroma of controls (*M*). □, peritumoral stroma, ■, mutant psoriasiform DMBA-treated skin, ▨, control tumor-free, DMBA-treated skin. §, $P < 0.0001$ for mutant DMBA-treated skin compared with control tumors. All skin samples were taken at 21–23 weeks after start of DMBA application.



healing and chemical carcinogenesis. VEGF-A is essential for embryonic blood vessel development (9, 10), but the lack of any major change in the dermal vasculature of *VEGF-A*$^{\Delta k5\text{-cre}/\Delta k5\text{-cre}}$ mice demonstrates that keratinocyte-derived VEGF-A is not essential for the establishment of the skin vasculature during embryogenesis and can probably be functionally substituted by either VEGF-A from other sources, such as Schwann cells of peripheral nerves (34) or other angiogenic factors, such as transforming growth factor $\beta$1, fibroblast growth factor 2, and the angiopoietins (35).

VEGF-A is an important factor in angiogenesis during wound healing and is strongly up-regulated in keratinocytes in skin wounds (14). However, the data presented in this study suggest that other sources in the early wound bed can substitute for keratinocyte-derived VEGF-A, for example, liberation from extracellular matrix stores by platelet-secreted proteases (36) or secretion by infiltrating macrophages. In addition, other proangiogenic cytokines, such as the fibroblast growth factors, platelet-derived growth factor, transforming growth factor $\beta$, and interleukin 8 (reviewed in Ref. 37) or keratinocyte-derived PlGF (38) and fibroblast growth factor 2 (39) could contribute to blood vessel formation in the early wound bed. By

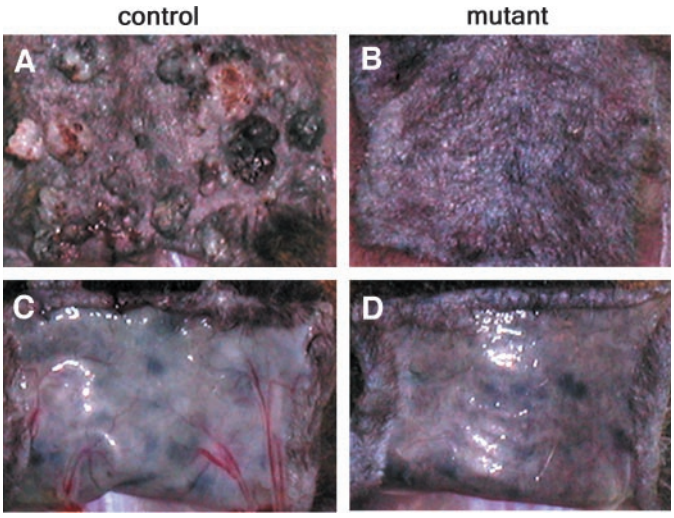


Fig. 7. Large s.c. blood vessels develop in association with papillomas, but not with inflamed or hyperkeratotic skin. *A* and *B* show the appearance of 9,12-dimethyl 1,2-benzanthracene-treated skin in examples of *VEGF-A*$^{loxP/loxP}$ (*control*) and *VEGF-A*$^{\Delta k5\text{-}cre/\Delta k5\text{-}cre}$ (*mutant*) mice after 23 and 21 weeks, respectively, whereas *C* and *D* show the dermal side of the skin.

contrast, during the completion of wound re-epithelialization, as evidenced by crust shedding (40, 41), keratinocytes may become the most important source of VEGF-A. Thus, in its absence, negative regulators of angiogenesis, such as thrombospondin-2 (20), which increases in the later stages of wound healing (42), could predominate, leading to capillary cell death and the formation of an avascular zone. In addition, VEGF-A acts as a chemotactic factor for endothelial cells (43), so that its absence in mutant mice might lead to decreased migration toward the epidermis, again resulting in a blood vessel-free zone. Keratinocyte-derived VEGF-A is therefore dispensable for the early phases of granulation tissue formation and angiogenesis but plays a role in the later phase of wound healing, namely, the *reconstitutio ad integrum* of the subepidermal capillary plexus. Furthermore, the lack of subepidermal capillaries implies that the action of keratinocyte-derived VEGF-A, be it survival or chemotactic, is targeted to the endothelial cells of these capillaries only and does not attract infiltrating macrophages, whose distribution during the course of healing did not correlate with the presence of keratinocyte-derived VEGF-A. Furthermore, these macrophages cannot substitute for keratinocyte-derived VEGF-A in the reconstitution of the subepidermal capillary plexus.

In contrast to the partial independence from keratinocyte-derived VEGF-A for normal skin biology and wound healing, our data demonstrate that the formation of DMBA-induced epidermal tumors crucially depends on VEGF-A produced by keratinocytes. It is well established that tumor growth above a certain size is dependent on angiogenesis and that VEGF-A is important for this process. Specifically, in skin, VEGF-A is up-regulated in premalignant papillomas (44), and targeted overexpression of VEGF-A to murine epidermis predisposes mice to the development of tumors (45). Furthermore, an increase in VEGF-A expression correlates directly with increased activity of oncogenes important in skin carcinogenesis (44, 46). Conversely, in a model of murine pancreatic $\beta$-cell carcinogenesis, loss of VEGF-A expression leads to a reduction of tumor numbers and size (47). In the model of skin carcinogenesis used in the present study, lack of VEGF-A expression in DMBA-treated mutant mouse skin did not merely result in smaller or fewer papillomas than in control animals but virtually abrogated papilloma development altogether. Moreover, dysplastic changes, although obvious in papillomas and SCCs of control mice, were at best indefinite, even within the most hyperplastic epidermis of the mutants, and blood vessel density was comparable with that of normal skin. Thus, in the multistage model of skin carcinogenesis, in which activation of oncogenes results in progression from hyperplasia to dysplasia with concomitant angiogenesis and finally to invasive carcinomas, keratinocyte VEGF-A-null mice are arrested at the predysplastic stage of hyperplasia. Dysplastic cells may have an increased metabolic rate compared with normal cells (48), and the increased vascularization induced by VEGF-A could provide the nutrients necessary for their survival and for the exophytic growth typical of papillomas. However, our finding that similar numbers of apoptotic cells were present in both hyperproliferative epidermis of mutant mice and tumor-free DMBA-treated skin of control mice argues against this interpretation and suggests that other mechanisms are involved in the suppression of tumor outgrowth in the absence of VEGF-A.

Mast cells have been suggested to "kick-start"' the angiogenic switch in the early stages of tumor development (33), perhaps providing the angiogenic stimulus even before the hyperplastic tissue itself. However, the finding that ample mast cells present in the vicinity of hyperplastic epidermis did not result in increased angiogenesis and papilloma development suggests that angiogenic factors produced by these cells are by themselves insufficient to induce the angiogenic switch.

The dependence of papilloma formation on keratinocyte-derived VEGF-A has been confirmed in a different mouse model, in which K5-SOS mice, which develop papillomas with 100% penetrance, were crossed to the VEGF-A$^{\Delta k5\text{-}cre/\Delta k5\text{-}cre}$ mice described here. Double transgenic mice bearing the *K5-SOS* and *cre* transgenes and thus lacking keratinocyte-derived VEGF-A were retarded in papilloma formation compared with K5-SOS controls.[7] Nevertheless, the mechanism underlying the almost complete abrogation of tumor formation deserves further study. For instance, lymphangiogenesis, which is also important for tumor formation and has recently been shown to be regulated by VEGF-A (49), has not yet been examined in this model, and a study of the behavior of inflammatory cells in the absence of VEGF-A during tumorigenesis may shed light on the chemotactic stimuli that these cells need to migrate.

In summary, we have investigated the contribution of epidermal keratinocyte-derived VEGF-A to two important settings of angiogenesis in the adult, namely, wound healing and tumor formation in the skin. We show that firstly, keratinocyte-derived VEGF-A is essential for re-establishment of the subepithelial capillary plexus in the late phase of wound healing and that in its absence, wound healing is substantially retarded. Promotion of VEGF-A secretion or application of VEGF-A-containing medication (reviewed in Ref. 50) may thus be an effective therapy in both the late and early phases of poorly healing wounds. Secondly, the lack of dysplastic cells in carcinogen-treated skin in the absence of VEGF-A suggests that this cytokine is not only important for growth of advanced tumors but might also be involved in the early phase of progression from the hyperplastic to the dysplastic stage.

## ACKNOWLEDGMENTS

We are grateful to Junji Takeda (Osaka University, Osaka, Japan) and Napoleone Ferrara (Genentech) for the kind gifts of the K5-*cre*$^{+}$ and *VEGF-A*$^{loxP/loxP}$ mice, respectively; to Jozef Ban for help with the Southern blotting; to Christoph Mayer, Chung-I Wu, and Barbara Lengauer for excellent technical assistance; and to the staff of the Biomedizinisches Zentrum, Medical University of Vienna for the care of the mice.

[7] B. Lichtenberger and M. Sibilia, unpublished results.

## REFERENCES


1. Ferrara N. Molecular and biological properties of vascular endothelial growth factor. J Mol Med 1999;77:527–43.
2. Neufeld G, Cohen T, Gengrinovitch S, Poltorak Z. Vascular endothelial growth factor (VEGF) and its receptors. FASEB J 1999;13:9–22.
3. Marconcini L, Marchio S, Morbidelli L, et al. c-fos-induced growth factor/vascular endothelial growth factor D induces angiogenesis in vivo and in vitro. Proc Natl Acad Sci USA 1999;96:9671–6.
4. Odorisio T, Schietroma C, Zaccaria ML, et al. Mice overexpressing placenta growth factor exhibit increased vascularization and vessel permeability. J Cell Sci 2002;115: 2559–67.
5. Jeltsch M, Kaipainen A, Joukov V, et al. Hyperplasia of lymphatic vessels in VEGF-C transgenic mice. Science (Wash DC) 1997;276:1423–5.
6. Dumont DJ, Jussila L, Taipale J, et al. Cardiovascular failure in mouse embryos deficient in VEGF receptor-3. Science (Wash DC) 1998;282:946–9.
7. DiSalvo J, Bayne ML, Conn G, et al. Purification and characterization of a naturally occurring vascular endothelial growth factor.placenta growth factor heterodimer. J Biol Chem 1995;270:7717–23.
8. Carmeliet P, Moons L, Luttun A, et al. Synergism between vascular endothelial growth factor and placental growth factor contributes to angiogenesis and plasma extravasation in pathological conditions. Nat Med 2001;7:575–83.
9. Carmeliet P, Ferreira V, Breier G, et al. Abnormal blood vessel development and lethality in embryos lacking a single VEGF allele. Nature (Lond) 1996;380:435–9.
10. Ferrara N, Carver-Moore K, Chen H, et al. Heterozygous embryonic lethality induced by targeted inactivation of the VEGF gene. Nature (Lond) 1996;380:439–42.
11. Ferrara N. VEGF: an update on biological and therapeutic aspects. Curr Opin Biotechnol 2000;11:617–24.
12. Ballaun C, Weninger W, Uthman A, Weich H, Tschachler E. Human keratinocytes express the three major splice forms of vascular endothelial growth factor. J Investig Dermatol 1995;104:7–10.
13. Weninger W, Uthman A, Pammer J, et al. Vascular endothelial growth factor production in normal epidermis and in benign and malignant epithelial skin tumors. Lab Investig 1996;75:647–57.
14. Brown LF, Yeo KT, Berse B, et al. Expression of vascular permeability factor (vascular endothelial growth factor) by epidermal keratinocytes during wound healing. J Exp Med 1992;176:1375–9.
15. Brown LF, Olbricht SM, Berse B, et al. Overexpression of vascular permeability factor (VPF/VEGF) and its endothelial cell receptors in delayed hypersensitivity skin reactions. J Immunol 1995;154:2801–7.
16. Brown LF, Harrist TJ, Yeo KT, et al. Increased expression of vascular permeability factor (vascular endothelial growth factor) in bullous pemphigoid, dermatitis herpetiformis, and erythema multiforme. J Investig Dermatol 1995;104:744–9.
17. Detmar M, Brown LF, Claffey KP, et al. Overexpression of vascular permeability factor/vascular endothelial growth factor and its receptors in psoriasis. J Exp Med 1994;180:1141–6.
18. Viac J, Palacio S, Schmitt D, Claudy A. Expression of vascular endothelial growth factor in normal epidermis, epithelial tumors and cultured keratinocytes. Arch Dermatol Res 1997;289:158–63.
19. Bikfalvi A, Klein S, Pintucci G, Rifkin DB. Biological roles of fibroblast growth factor-2. Endocr Rev 1997;18:26–45.
20. Detmar M. The role of VEGF and thrombospondins in skin angiogenesis. J Dermatol Sci 2000;24(Suppl 1):S78–84.
21. Suri C, McClain J, Thurston G, et al. Increased vascularization in mice overexpressing angiopoietin-1. Science (Wash DC) 1998;282:468–71.
22. Fukumura D, Xavier R, Sugiura T, et al. Tumor induction of VEGF promoter activity in stromal cells. Cell 1998;94:715–25.
23. Sauer B. Inducible gene targeting in mice using the Cre/lox system. Methods: A Companion to Methods Enzymol 1998;14:381–92.
24. Tarutani M, Itami S, Okabe M, et al. Tissue-specific knockout of the mouse Pig-a gene reveals important roles for GPI-anchored proteins in skin development. Proc Natl Acad Sci USA 1997;94:7400–5.
25. Gerber HP, Hillan KJ, Ryan AM, et al. VEGF is required for growth and survival in neonatal mice. Development (Camb) 1999;126:1149–59.
26. Hager B, Bickenbach JR, Fleckman P. Long-term culture of murine epidermal keratinocytes. J Investig Dermatol 1999;112:971–6.
27. Thompson EM, Legouy E, Renard JP. Mouse embryos do not wait for the MBT: chromatin and RNA polymerase remodeling in genome activation at the onset of development. Dev Genet 1998;22:31–42.
28. Mecklenburg L, Nakamura M, Ellerbrok H, Tobin DJ, Paus R. Hair cycle-dependent expression of VEGF-splice variants in murine skin suggests key functions in the regulation of perifollicular microvascular remodelling [abstract]. Arch Dermatol Res 2002;294:70.
29. Yano K, Brown LF, Detmar M. Control of hair growth and follicle size by VEGF-mediated angiogenesis. J Clin Investig 2001;107:409–17.
30. Ruggeri B, Caamano J, Slaga TJ, et al. Alterations in the expression of uvomorulin and $Na^{+}$,$K(^{+})$-adenosine triphosphatase during mouse skin tumor progression. Am J Pathol 1992;140:1179–85.
31. Luttun A, Tjwa M, Moons L, et al. Revascularization of ischemic tissues by PlGF treatment, and inhibition of tumor angiogenesis, arthritis and atherosclerosis by anti-Flt1. Nat Med 2002;8:831–40.
32. Pasparakis M, Courtois G, Hafner M, et al. TNF-mediated inflammatory skin disease in mice with epidermis-specific deletion of IKK2. Nature (Lond) 2002;417:861–6.
33. Coussens LM, Raymond WW, Bergers G, et al. Inflammatory mast cells up-regulate angiogenesis during squamous epithelial carcinogenesis. Genes Dev 1999;13:1382–97.
34. Mukouyama YS, Shin D, Britsch S, Taniguchi M, Anderson DJ. Sensory nerves determine the pattern of arterial differentiation and blood vessel branching in the skin. Cell 2002;109:693–705.
35. Beck L Jr, D'Amore PA. Vascular development: cellular and molecular regulation FASEB J 1997;11:365–73.
36. Houck KA, Leung DW, Rowland AM, Winer J, Ferrara N. Dual regulation of vascular endothelial growth factor bioavailability by genetic and proteolytic mechanisms. J Biol Chem 1992;267:26031–7.
37. Tonnesen MG, Feng X, Clark RA. Angiogenesis in wound healing. J Investig Dermatol Symp Proc 2000;5:40–6.
38. Failla CM, Odorisio T, Cianfarani F, et al. Placenta growth factor is induced in human keratinocytes during wound healing. J Investig Dermatol 2000;115:388–95.
39. Kurita Y, Tsuboi R, Ueki R, Rifkin DB, Ogawa H. Immunohistochemical localization of basic fibroblast growth factor in wound healing sites of mouse skin. Arch Dermatol Res 1992;284:193–7.
40. Kyriakides TR, Tam JW, Bornstein P. Accelerated wound healing in mice with a disruption of the thrombospondin 2 gene. J Investig Dermatol 1999;113:782–7.
41. Zahir M. Formation of scabs on skin wounds. Br J Surg 1965;52:376–80.
42. Agah A, Kyriakides TR, Lawler J, Bornstein P. The lack of thrombospondin-1 (TSP1) dictates the course of wound healing in double-TSP1/TSP2-null mice. Am J Pathol 2002;161:831–9.
43. Waltenberger J, Claesson-Welsh L, Siegbahn A, Shibuya M, Heldin CH. Different signal transduction properties of KDR and Flt1, two receptors for vascular endothelial growth factor. J Biol Chem 1994;269:26988–95.
44. Larcher F, Robles AI, Duran H, et al. Up-regulation of vascular endothelial growth factor/vascular permeability factor in mouse skin carcinogenesis correlates with malignant progression state and activated H-ras expression levels. Cancer Res 1996; 56:5391–6.
45. Larcher F, Murillas R, Bolontrade M, Conti CJ, Jorcano JL. VEGF/VPF overexpression in skin of transgenic mice induces angiogenesis, vascular hyperpermeability and accelerated tumor development. Oncogene 1998;17:303–11.
46. Baudino TA, McKay C, Pendeville-Samain H, et al. c-Myc is essential for vasculogenesis and angiogenesis during development and tumor progression. Genes Dev 2002;16:2530–43.
47. Inoue M, Hager JH, Ferrara N, Gerber HP, Hanahan D. VEGF-A has a critical, nonredundant role in angiogenic switching and pancreatic beta cell carcinogenesis. Cancer Cell 2002;1:193–202.
48. Drezek R, Brookner C, Pavlova I, et al. Autofluorescence microscopy of fresh cervical-tissue sections reveals alterations in tissue biochemistry with dysplasia. Photochem Photobiol 2001;73:636–41.
49. Nagy JA, Vasile E, Feng D, et al. Vascular permeability factor/vascular endothelial growth factor induces lymphangiogenesis as well as angiogenesis. J Exp Med 2002; 196:1497–506.
50. Dvorak HF. Vascular permeability factor/vascular endothelial growth factor: a critical cytokine in tumor angiogenesis and a potential target for diagnosis and therapy. J Clin Oncol 2002;20:4368–80.